Approaching the limit of electromechanical performance in mixed-phase nanocomposites

Article (Accepted Version)

Approaching the Limit of Electromechanical Performance in Mixed-Phase Nanocomposites

Conor S Boland*

School of Mathematical and Physical Sciences, University of Sussex, Brighton, BN1 9QH, United Kingdom

*c.s.boland@sussex.ac.uk

Abstract

Electrically conductive polymer-based nanocomposites have displayed excellent performances when applied as strain sensors for bodily monitoring. Among the most common form of these systems is the mixed-phased nanocomposite. Through a simple model that combines electromechanical and percolation theory it is reported here that in comparative systems, 2-dimensional nanofillers exhibit a larger electromechanical response than their 1-dimensional counterparts. For both nanofiller types, electromechanical response was found to increase greatly with aspect ratio and when shifting from an isotropic to anisotropic system. Furthermore, nanocomposites with bulk dimensions intrinsically outperform thinner systems theorised to be based on ink printing production methods.

Keywords: mixed-phase, nanocomposite, aspect ratio, 2D materials, 1D materials, strain sensor, bodily sensor

Introduction

Polymer-based mixed-phase nanocomposites are one of the most highly researched aspects of materials science to date.[1] Most commonly, these composite materials are formed through simple solution processing, whereby a dispersion of nanomaterial such carbon nanotubes (CNTs) or graphene are mixed with a polymer solution. This mixture can then be cast into a molding or filtered to form a nanocomposite film with nanofillers mixed into the polymer matrix (See Figure 1). At very low loading levels of nanofiller, polymers are reported to display large increases in mechanical properties.[2] At a critical loading level, polymers transition from electrically insulting to conductive behaviour in accordance with percolation theory[3]

$$\sigma_{\varepsilon=0} = \sigma_f(\varphi_f - \varphi_0)^t \quad (1)$$

Where $\sigma_{\varepsilon=0}$ is the zero-strain nanocomposite conductivity, σ_f is the apparent conductivity of the nanofiller, φ_f is the volume fraction of nanofiller, φ_0 is the percolation threshold volume fraction and t is the percolation exponent. Elastomer-based conductive nanocomposites using a range of nanofillers are reported to have reversible, strain sensitive electrical properties and have successfully been demonstration by researchers as strain sensing materials that can applied as bodily monitors.[4] Being highly sensitive to even the most minute deformation, their effectiveness at measuring a range of vital sign signals is unmatched by current commercial sensors. As these nanocomposites are based on cheap starting materials and with their cost/time efficient mode of liquid-based production, they are heralded as one of the great hopes for the commercial application of nanotechnologies.[5]

The electromechanical response of all mixed-phase nanocomposite strain sensors, generally taking the form of fractional resistance change ($\Delta R/R_0$) as a function of strain (ε), can be broken down into two distinct regions.[4] Beginning at low strain, an elastic linear regime is found where $\Delta R/R_0$ is related to ε through the electromechanical sensitivity metric, the gauge factor (G), by[6]

$$\frac{\Delta R}{R_0} = G\varepsilon$$

(2)

To note, low strain is not a performance criterion or system limitation but an important distinction that has to be made when describing how one goes about understanding performance and thus the extrapolation of intrinsic performance metrics.[4] For a particular nanocomposite system with a specific volume fraction of nanofiller, *G* will be constant. In this linear region, resistance change exhibited by the bulk nanocomposite is due to tunnelling resistance between nanofillers changing as a result of decreasing cross-sectional area overlap of nanofillers with applied strain.[4] Through Simmons,[7] an approach to approximately derive the tunnelling resistance between nanofillers in a composite system was shown as

$$R_t = \frac{h^2 d}{A e_m^2 \sqrt{2m\lambda}} e^{\frac{4\pi d}{h}\sqrt{2m\lambda}}$$

(3)

Where R_t, h, d, A, e_m, m and λ are the tunnelling resistance, Plank's constant, tunnelling distance, cross-sectional area, electron charge, electron mass and potential barrier height respectively. From this expression an inverse proportionality between tunnelling resistance and areal overlap is seen. The linear relationship in eq 2 is satisfied as long as the strains experienced by the nanocomposite are below the yield strain of the material.[4] Below the yield point, changes in the distribution of d from eq 3 due to viscoplastic flow of nanofillers are minimised, leading to a linear electromechanical response dominated by changes in nanofiller areal overlap.[4, 8] The linear limit of a material's response is set by the yield strain and can be described using the linear range metric, the working factor (*W*).[4] Repeated cycles in this linear regime are reported to follow a regular and well-defined power law decay until a critical number of conditioning cycles, known as the endurance limit, is reached after which a steady state signal is observed.[9] Beyond the yield point and *W*, nanocomposites will undergo plastic deformation and their response will be non-linear due to the tunnelling distance between nanofillers changing.[4] From the right-hand side of eq 3, it can be seen that a non-linear, exponential increase in

tunnelling resistance will occur with increasing tunnelling distance. It is this mechanism that will start to dominate electromechanical response. To truly unlock the commercial potential of these materials it is prudent that we as researchers understand what controls electromechanical performance and how best to maximise it. Many models exist that describe the response curve of nanocomposites but in most cases are empirical and unique to that particular material.[10, 11] Furthermore, past emphasis on fitting the whole response curve[12] including the plastic regime, for the most part, is redundant as it is outside of the functional working range of a nanocomposite. Strains beyond *W* cannot be practically applied in applications that require repeatable measurement, as signal is reported to be highly irregular.[9] Thus, a simple, more universal mode of modelling, which focuses on describing the linear regime and incorporating nanocomposite network properties to describe electromechanical performance is required.

Here we report a simple model that combines percolation and electromechanical theory to project the electromechanical response of mixed-phase nanocomposites. Through this model the physical geometric dimensions of a nanocomposite and its respective nanofiller can be incorporated into the projection of performance. Vitally, this model facilitates narrowing the research focus and increasing the commercialisable potential of sensor research by identifying how nanofiller aspect ratio and nanocomposite thickness maximises performance. To the author's knowledge, no prior model takes into consideration the effects aspect ratio and nanocomposite geometrics have on electromechanical performance. The approach for our model here is one that relies on an introspective, analytical methodology which utilises trends and results reported in literary data. In the past, such an approach has been successful in identifying critical intrinsic material properties that greatly influence a nanocomposite's strain sensing performance.[4, 9] Furthermore, dissimilar to previous models, here the ramifications of nanocomposite functional application strain range is considered.

Results and Discussion

A more complete understanding of electromechanical response in mixed-phase nanocomposites can begin through a simple modification of eq 2. It is seen that a relationship between resistance change (ΔR) and $\sigma_{\varepsilon=0}$ can be formed through the zero-strain nanocomposite resistance (R_0) using the following

$$\sigma_{\varepsilon=0} = \frac{L_0}{R_0 A_0}$$

(4)

Where A_0 and L_0 are constants associated with the nanocomposites cross-sectional area and gauge length respectively at zero-strain. Eq 2 can be plugged in and the following expression is formed

$$\rightarrow \sigma_{\varepsilon=0} = \left(\frac{G\varepsilon}{\Delta R}\right)\frac{L_0}{A_0}$$

(5)

Alternatively, eq 5 can be rearranged as resistance change (ΔR) as a function of ε

$$\rightarrow \Delta R = \left(\frac{GL_0}{A_0\sigma_{\varepsilon=0}}\right)\varepsilon$$

(6)

Where G and $\sigma_{\varepsilon=0}$ are constants for a nanocomposite of a given φ_f. Eq 5 is surprisingly a very power and simple express that essentially reflects what is universally reported for nanocomposite strain sensors, conductivity is inversely proportionally to resistance change.[4] Alternatively, in eq 6, for a large change in nanocomposite resistance to occur with applied strain, indicative of a large gauge factor, intrinsically conductivity will be low. This also implies that nanocomposite strain sensors will display their largest electromechanical response around φ_o, *i.e.* when nanocomposite conductivity is near its lowest.[13] To note, in terms of application, nanocomposites with low conductivity can be problematic for electrical engineering and signal processing due to increased signal noise at $\sigma_{\varepsilon=0} < 10^{-6}$ S/m.[14] Interesting, eq 6 suggests that there is a nanocomposite dimensionality dependence associated with ΔR. Essentially, if the dimensions of a nanocomposite system change, the volume in which the nanofillers occupy in the polymer matrix will in turn change. Previously, $\ln(\sigma_{\varepsilon=0})$ of a nanocomposite was reported

to scale linearly with the volume fraction of nanofiller as $-\varphi_f^{-1/3}$.[15, 16] Through analogy with the above, from eq 6, $1/\Delta R$ can be said to be proportional to $-\varphi_f^{-1/3}$. This is reflective of increases in φ_f being widely reported to result in a decrease in the value of G.[17] The cause of this decrease is due to the subsequent increase in nanofiller network connectivity leading to decreases in tunnelling distance and thus tunnelling resistance.[4] Tunnelling distance is said to be proportional to loading through the following[16]

$$d \propto -\varphi_f^{-1/3} \quad (7)$$

Through the author's previous work,[4] a simple expression which related G to W and a nanofiller alignment parameter (n_e) was shown. Through this expression, the magnitude of a nanocomposite's value for G is found to be highly reliant on these two nanocomposite properties.

$$G = 2 + \frac{n_e}{W} \quad (8)$$

It was previously reported that an increased value of n_e corresponded to a nanofiller network that was increasingly more anisotropic and aligned in-plane with respect to current flow. Other past studies[18] and mathematical models[19] also corroborate a connection between large G values and nanofiller alignment. As W is governed purely by the mechanics of the nanocomposite system and is a material constant independent of φ_f,[4] changes in G must be dominated by n_e. As eq 8 doesn't account for changes in G associated with φ_f, it implies n_e is dependent on tunnelling distance changes associated with alignment and thus φ_f (through eq 7) which in turn effect ΔR and $\sigma_{\varepsilon=0}$. These factors are particularly important to consider as φ_o in nanocomposites systems will trend toward larger values when nanofiller networks shift from isotropic to anisotropic.[20, 21]

We can reflect the findings of above by combining eq 1 and 5 to form the following expression

$$\left(\frac{GL_0}{A_0}\right)\frac{\varepsilon}{\Delta R} = \sigma_e(\varphi_f - \varphi_0)^t$$

(9)

Eq 9 can be rearranged to form a relationship which unifies electromechanical theory and sensitivity in the form of ΔR with nanocomposite dimensionality and percolation theory

$$\Delta \mathrm{R} = \left(\frac{\mathrm{L_0 G}}{\mathrm{A_0} \left[\sigma_f \left(\varphi_f - \varphi_0 \right)^t \right]} \right) \varepsilon$$

(10)

This expression should describe the linear elastic response of a nanocomposite beginning at low strain and ending at $\varepsilon = W$. Eq 10 was applied effectively to a range of nanocomposite systems from literature using both 2-dimensional (2D) and 1-dimensional (1D) nanofillers, graphene and multiwalled carbon nanotubes (MWCNTs) respectively. In Figure 2, eq 10 is found to fit the linear regime of the literary data accurately (see Supporting Information Table S1 for fit parameters). To note, this model is limited to the understanding and projection of only percolative mixed-phased nanocomposites systems. After now quantifying the connection between mixed-phase nanocomposite electromechanical response and material characteristics associated with nanocomposite conductivity, dependence on nanofiller aspect ratio can be drafted into the expression. The φ_0 of a mixed-phase nanocomposite system containing well dispersed randomly orientated nanofillers that are roughly ellipsoid in shape can be approximated geometrically through the inverse of nanofiller aspect ratio.[22] For prolate ellipsoids (*i.e.* 1D rod-like nanofillers), percolation threshold can be described as

$$\varphi_{0,\mathrm{rod}} = 0.6 \frac{\mathrm{D}}{\mathrm{L}}$$

(11)

Where *D* is the diameter of the rod-like ellipsoid and *L* the length (see top left inset in Figure 3). For oblate ellipsoids (*i.e.* 2D disk-like nanofillers) the percolation threshold can be said to be

$$\varphi_{0,\mathrm{disk}} = 1.27 \frac{\mathrm{D}}{\mathrm{L}}$$

(12)

Where *D* is the thickness of the disk-like ellipsoid and *L* the lateral length (see top left inset in Figure 3). Despite the assumptions, these expressions quite accurately predict the φ_o of mixed-phase nanocomposites quite accurately (see Supporting Information Table S2 for examples). From eqs 11 and 12, it is expected that φ_o will decrease with aspect ratio.[23] From substituting eq 11 and 12 into eq 10 for φ_o, now designated as $\varphi_{o,\,type}$ where type denotes rod or disk dimensions, an expression that includes ΔR dependence on nanofiller type and aspect ratio can now be formed.

$$\Delta \mathrm{R} = \left(\frac{\mathrm{L_0 G}}{\mathrm{A_0} \left[\sigma_f \left(\varphi_f - \varphi_{0,type} \right)^t \right]} \right) \varepsilon$$

(12)

We can see from eq 12 that resistance change scales with *G* and filler network parameters. This expression is only valid when $\varepsilon \leq W$, *i.e.* within the initial linear elastic regime. Thus eq 12 can be simplified by replacing ε with *W*

$$\Delta \mathrm{R} = \frac{\mathrm{W L_0 G}}{\mathrm{A_0} \left[\sigma_f \left(\varphi_f - \varphi_{0,type} \right)^t \right]}$$

(13)

From this expression ΔR is predicted to linearly increase with *G* and for both to intuitively vary with φ_f. Thus, a good representation of the measure of electromechanical response at low φ_f around electrical percolation can be given by $d\Delta R/dG$.

$$\frac{\mathrm{d}\Delta \mathrm{R}}{\mathrm{dG}} = \frac{\mathrm{W L_0}}{\mathrm{A_0} \left[\sigma_f \left(\varphi_f - \varphi_{0,type} \right)^t \right]}$$

(14)

The power of this expression lies in its predictive nature and its ability to be used to project electromechanical performance. Using an archetypical ideal nanocomposite system of dimensions L_0 = 0.01 m and a cross-sectional area of 10^{-6} m^2 (width of 0.01 m and thickness of 100μm), through eq 14, the electromechanical performance of 2D and 1D nanofillers and their isotropic and anisotropic systems can be compared. A nominal value of $W = 0.1$ was used for the modelling. For an isotropic system with bulk dimensions of ≥100μm,[8, 24, 25] the percolation exponent is a universal constant of $t \sim 2$, indicative of 3-dimensional charge transport through the nanocomposite.[26] The claim of universality though does come with some contention as values of t have been reported to decrease with aspect ratio of nanofiller.[27, 28] Conversely, there are also uncertainties associated with these reports as values of $t \sim 2$ have also been observed in nanocomposites with large[3] and small[29] aspect ratio fillers. Thus, for simplicity, the model here will assume t to be constant with aspect ratio. However, for anisotropic systems, the values of t are reported to increase roughly two-fold[20, 29, 30] and can thus be used to predict the electromechanical behaviour of aligned nanofiller systems. Graphene and CNTs, reported to be the most commonly applied nanofillers in literature for nanocomposite strain sensors,[4] are used here as the typical 2D and 1D fillers. For these two nanomaterials, liquid phase exfoliated networks are reported to have σ_f values of ~10^4 S/m and ~10^5 S/m for graphene[31] and CNTs[32] respectively. With respect to filler alignment [33, 34] and aspect ratio,[35-39] σ_f is reported not to vary significantly. φ_o for isotropic systems are calculated using a range of aspect ratios and eqs 11 and 12. For anisotropic systems, previous studies found that φ_o increased on average two-fold in 2D and 1D nanofiller systems,[40-44] allowing the anisotropic φ_o to be projected. As previously stated, nanocomposites are most sensitive when loading levels are near φ_o, thus for all modelling φ_f was a constant value of $1.05\varphi_o$ (*i.e.* 5% above φ_o). For a list of fit parameter constants, see Supporting Information Table S3.

Using the above fit parameters, in Figure 3, calculated values of $d\Delta R/dG$ for bulk isotropic and anisotropic nanocomposite systems using both 2D and 1D nanofillers where plotted as a function of aspect ratio (L/D). Firstly, it is noted that electromechanical response increases greatly with aspect ratio and is reflective of previous reports which showed similar increases when varying the aspect ratio of 2D[45] and 1D[46-48] nanofillers in a range of nanocomposite systems. This finding implies that a decreased

number of connections in a nanofiller network brought about by larger aspect ratios and thus a high degree of exfoliation equality are two of the dominate properties which can govern nanocomposite electromechanical response. In both orientation cases, 2D nanofillers are noted to perform better than their 1D counterpart. Previously, it was reported that experimentally graphene-based nanocomposite strain sensors on average displayed values of G larger than CNT-based ones.[4] A model by Yao *et al.* also predicts that graphene based mixed-phase nanocomposites will have larger G values than CNT systems.[49] For the isotropic systems, the 2D nanofiller has an electromechanical response that is five-times larger than the 1D nanofiller. This discrepancy is even bigger in the anisotropic systems, with the 2D nanofiller reported here to have a response nearly two orders of magnitude larger than the 1D nanofiller. As previously predicted from eq 8, in comparison with isotropic systems, the anisotropic ones are confirmed to have a larger electromechanical response. For nanofillers with $L/D \sim 1000$, the 2D anisotropic system had a response eight orders of magnitude larger than the isotropic one.

Liquid phase exfoliation is widely used to prepare many types of nanofiller.[50] Solution processing of nanocomposites is the dominate mode of production and it is to no surprise that research recently has been treading towards applying nanocomposite inks (*i.e.* nanofiller and polymer solution mixed) for a wide range of printing methods.[50] The advantage of these methods is that nanocomposites of small feature size and thickness can be produced. Looking at the electromechanical response dependence on nanocomposite thickness using eq 14, we can assume a system similar to before with the exception of a decreased thickness of 5μm. For the thin layer systems, σ_f will remain the same for both nanofiller types as above 50nm, networks of graphene and CNTs are reported to have bulk-like conductivity.[51] As these system are so thin however, we can assume that the percolation exponent will be nearer to a universal value of ~1.3,[52-54] indicative of 2D charge transport through the nanocomposite.[26] In Figure 4A, thin isotropic nanocomposite layers are compared to the previous thicker, bulk isotropic systems. From plotting the bulk and layered nanocomposites against one another, at $L/D \geq 1000$, bulk systems display performances that are on average two orders of magnitude larger. For $L/D < 1000$, performances converge. However, response is still an order of magnitude larger for the bulk systems even at $L/D \sim$

100. For the thin layer systems, 2D nanofillers are again found to perform the best, with their electromechanical response a factor of three better than the 1D nanofillers.

Similar to before, comparing isotropic and anisotropic layer nanocomposites in Figure 4B sees the anisotropic systems displaying a larger electromechanical response. 2D nanofillers again are found to show the better performance. At a nominal $L/D \sim 1000$, the anisotropic 2D system has a response five orders of magnitude larger than the isotropic one. This value difference however, is slightly lower than what was see when coming the bulk isotropic and anisotropic systems. From plotting the anisotropic bulk and layered systems against each other in Figure 5, at $L/D \sim 1000$ the bulk 2D system has an electromechanical response two orders of magnitude larger than its thin layer counterpart. This in fact runs many parallels with previous reports on printed nanocomposites[54-56] and pristine nanomaterials[57] where G was found to increase with layer number and overall deposition thickness. At $L/D < 1000$, electromechanical response is seen to converge until a cross-over point of $L/D \sim 50$ where the bulk and layer values for the respective materials have similar values.

Conclusions

We can conclude that the findings of this work suggest that bulk anisotropic nanocomposites based on 2D nanofillers have superior electromechanical response. However, it is the processability of these and other types of nanocomposites that will dictate the feasibility of such a conclusion. Currently, due to a lack of experimental data, it is unclear if anisotropic bulk or thin layered nanocomposites are easier to produce and if other nanocomposite properties, mainly mechanical, will support application. For scalable inkjet and spray coating methods, applying nanosheets with large aspect ratios would be an issue as lateral size is restricted to being $1/50^{th}$ the size of the nozzle diameter.[58] In many cases, this results in nanosheets needing to be <400 nm in lateral size to prevent clogging of the nozzle[59, 60] and resulting in $L/D < 400$, which would result in lowered electromechanical response. This also does not take into account viscosity changes in the ink as a result of the presence of the polymer which will effect printability. It is also unknown how a subsequent dilution step, a common method of counteracting viscosity changes, will effect processing time and heterostructure. Conclusively, larger aspect ratio fillers display the best electromechanical performance however, when taking nanocomposite mechanics

into account, modulus is known to steeply increase with aspect ratio.[61] As noted in the author's prior work, to function as a skin-on bodily sensors, nanocomposites must have moduli approaching that of human skin and ligaments.[4] This is a catch-22 research now faces but is an uncertainly that can be answered with further investigation.

Supporting Information

Supporting Information includes Tables S1, S2 and S3. This Supporting Information is available online free of charge.

Acknowledgements

This work was supported by strategic development funding from the University of Sussex.

References

1. Kinloch, I. A.; Suhr, J.; Lou, J.; Young, R. J.; Ajayan, P. M. Composites with carbon nanotubes and graphene: An outlook. *Science* **2018,** 362, (6414), 547-553.
2. Papageorgiou, D. G.; Kinloch, I. A.; Young, R. J. Mechanical properties of graphene and graphene-based nanocomposites. *Prog. Mater. Sci.,* **2017,** 90, 75-127.
3. Boland, C. S.; Khan, U.; Backes, C.; O'Neill, A.; McCauley, J.; Duane, S.; Shanker, R.; Liu, Y.; Jurewicz, I.; Dalton, A. B.; *et al.* Sensitive, high-strain, high-rate bodily motion sensors based on graphene-rubber composites. *ACS Nano* **2014,** 8, (9), 8819-30.
4. Boland, C. S. Stumbling through the Research Wilderness, Standard Methods To Shine Light on Electrically Conductive Nanocomposites for Future Healthcare Monitoring. *ACS Nano* **2019,** 13, (12), 13627-13636.
5. 2019 Annual Report, Graphene Flagship
6. Boland, C. S.; Khan, U.; Ryan, G.; Barwich, S.; Charifou, R.; Harvey, A.; Backes, C.; Li, Z.; Ferreira, M. S.; Mobius, M. E.; *et al.* Sensitive Electromechanical Sensors Using Viscoelastic Graphene-Polymer Nanocomposites. *Science* **2016,** 354, (6317), 1257-1260.
7. Simmons, J. G. Generalized Formula for the Electric Tunnel Effect between Similar Electrodes Separated by a Thin Insulating Film. *J. Appl. Phys.* **1963,** 34, (6), 1793-1803.
8. Hu, N.; Karube, Y.; Yan, C.; Masuda, Z.; Fukunaga, H. Tunneling effect in a polymer/carbon nanotube nanocomposite strain sensor. *Acta. Mater.* **2008,** 56, (13), 2929-2936.
9. Boland, C. S. Quantifying the Contributing Factors toward Signal Fatigue in Nanocomposite Strain Sensors. *ACS Appl. Polym. Mater.* **2020,** 2, (8), 3474-3480.
10. Wang, X.; Meng, S.; Tebyetekerwa, M.; Li, Y.; Pionteck, J.; Sun, B.; Qin, Z.; Zhu, M. Highly sensitive and stretchable piezoresistive strain sensor based on conductive poly(styrene-butadiene-styrene)/few layer graphene composite fiber. *Composites, Part A,* **2018,** 105, 291-299.
11. Liu, H.; Li, Y.; Dai, K.; Zheng, G.; Liu, C.; Shen, C.; Yan, X.; Guo, J.; Guo, Z. Electrically conductive thermoplastic elastomer nanocomposites at ultralow graphene loading levels for strain sensor applications. *J. Mater. Chem. C* **2015,** 4, (1), 157-166.
12. Kumar, A. Electrical Percolation in Metal Wire Network-Based Strain Sensors. *IEEE Sens. J.* **2019,** 19, (22), 10373-10378.

13. O'Driscoll, D. P.; Vega-Mayoral, V.; Harley, I.; Boland, C. S.; Coleman, J. N. Optimising composite viscosity leads to high sensitivity electromechancial sensors. *2D Mater.* **2018,** 5, (3), 035042.
14. Chung, D. D. L. Electrical applications of carbon materials. *J. Mater. Sci.* **2004,** 39, (8), 2645-2661.
15. Kilbride, B. E.; Coleman, J. N.; Fraysse, J.; Fournet, P.; Cadek, M.; Drury, A.; Hutzler, S.; Roth, S.; Blau, W. J. Experimental observation of scaling laws for alternating current and direct current conductivity in polymer-carbon nanotube composite thin films. *J. Appl. Phys.* **2002,** 92, (7).
16. Maiti, S.; Suin, S.; Shrivastava, N. K.; Khatua, B. B. Low percolation threshold in polycarbonate/multiwalled carbon nanotubes nanocomposites through melt blending with poly(butylene terephthalate). *J. Appl. Polym. Sci.* **2013,** 130, (1), 543-553.
17. Pham, G. T.; Park, Y.-B.; Liang, Z.; Zhang, C.; Wang, B. Processing and modeling of conductive thermoplastic/carbon nanotube films for strain sensing. *Composites, Part B* **2008,** 39, (1), 209-216.
18. Pu, J. H.; Zha, X. J.; Zhao, M.; Li, S.; Bao, R. Y.; Liu, Z. Y.; Xie, B. H.; Yang, M. B.; Guo, Z.; Yang, W. 2d End-to-End Carbon Nanotube Conductive Networks in Polymer Nanocomposites: A Conceptual Design to Dramatically Enhance the Sensitivities of Strain Sensors. *Nanoscale* **2018,** 10, (5), 2191-2198.
19. Theodosiou, T. C.; Saravanos, D. A. Numerical investigation of mechanisms affecting the piezoresistive properties of CNT-doped polymers using multi-scale models. *Compos. Sci. Technol.* **2010,** 70, (9), 1312-1320.
20. Li, C.; Chou, T.-W. Electrical Conductivities of Composites with Aligned Carbon Nanotubes. *J. Nanosci. Nanotechnol.* **2009,** 9, (4), 2518-2524.
21. Felisberto, M.; Arias-Durán, A.; Ramos, J. A.; Mondragon, I.; Candal, R.; Goyanes, S.; Rubiolo, G. H. Influence of filler alignment in the mechanical and electrical properties of carbon nanotubes/epoxy nanocomposites. *Phys. B* **2012,** 407, (16), 3181-3183.
22. Garboczi, E. J.; Snyder, K. A.; Douglas, J. F.; Thorpe, M. F. Geometrical percolation threshold of overlapping ellipsoids. *Phys. Rev. E* **1995,** 52, (1), 819-828.
23. Li, J.; Kim, J.-K. Percolation threshold of conducting polymer composites containing 3D randomly distributed graphite nanoplatelets. *Compos. Sci. Technol.* **2007,** 67, (10), 2114-2120.
24. Wang, B.; Lee, B.-K.; Kwak, M.-J.; Lee, D.-W. Graphene/polydimethylsiloxane nanocomposite strain sensor. *Rev. Sci. Instrum.* **2013,** 84, (10), 105005.
25. Zhao, H.; Bai, J. Highly Sensitive Piezo-Resistive Graphite Nanoplatelet–Carbon Nanotube Hybrids/Polydimethylsilicone Composites with Improved Conductive Network Construction. *ACS Appl. Mater. Interfaces* **2015,** 7, (18), 9652-9659.
26. Marsden, A. J.; Papageorgiou, D. G.; Vallés, C.; Liscio, A.; Palermo, V.; Bissett, M. A.; Young, R. J.; Kinloch, I. A. Electrical percolation in graphene–polymer composites. *2D Mater.* **2018,** 5, (3), 032003.
27. Ram, R.; Rahaman, M.; Aldalbahi, A.; Khastgir, D. Determination of percolation threshold and electrical conductivity of polyvinylidene fluoride (PVDF)/short carbon fiber (SCF) composites: effect of SCF aspect ratio. *Polym. Int.* **2017,** 66, (4), 573-582.
28. Xu, W.; Su, X.; Jiao, Y. Continuum percolation of congruent overlapping spherocylinders. *Phys. Rev. E* **2016,** 94, (3), 032122.
29. Dalmas, F.; Dendievel, R.; Chazeau, L.; Cavaillé, J.-Y.; Gauthier, C. Carbon nanotube-filled polymer composites. Numerical simulation of electrical conductivity in three-dimensional entangled fibrous networks. *Acta. Mater.* **2006,** 54, (11), 2923-2931.
30. Yao, H.; Hsieh, Y.-P.; Kong, J.; Hofmann, M. Modelling electrical conduction in nanostructure assemblies through complex networks. *Nat. Mater.* **2020,** 19, (7), 745-751.
31. De, S.; King, P. J.; Lotya, M.; O'Neill, A.; Doherty, E. M.; Hernandez, Y.; Duesberg, G. S.; Coleman, J. N. Flexible, Transparent, Conducting Films of Randomly Stacked Graphene from Surfactant-Stabilized, Oxide-Free Graphene Dispersions. *Small* **2010,** 6, (3), 458-464.
32. De, S.; Lyons, P. E.; Sorel, S.; Doherty, E. M.; King, P. J.; Blau, W. J.; Nirmalraj, P. N.; Boland, J. J.; Scardaci, V.; Joimel, J.; *et al.* Transparent, Flexible, and Highly Conductive Thin Films Based on Polymer−Nanotube Composites. *ACS Nano* **2009,** 3, (3), 714-720.

33. Lu, X.; Yvonnet, J.; Detrez, F.; Bai, J. Low electrical percolation thresholds and nonlinear effects in graphene-reinforced nanocomposites: A numerical analysis. *J. Compos. Mater.* **2018,** 52, (20), 2767-2775.
34. Bao, W. S.; Meguid, S. A.; Zhu, Z. H.; Meguid, M. J. Modeling electrical conductivities of nanocomposites with aligned carbon nanotubes. *Nanotechnology* **2011,** 22, (48), 485704.
35. Zhang, Y.; Li, H.; Liu, P.; Peng, Z. In *Study on electrical properties and thermal conductivity of carbon nanotube/epoxy resin nanocomposites with different filler aspect ratios*, 2016 *IEEE I.C.H.V.E.*, 1-4.
36. Kumar, P.; Yu, S.; Shahzad, F.; Hong, S. M.; Kim, Y.-H.; Koo, C. M. Ultrahigh electrically and thermally conductive self-aligned graphene/polymer composites using large-area reduced graphene oxides. *Carbon* **2016,** 101, 120-128.
37. Kratochvíla, J.; Boudenne, A.; Krupa, I. Effect of filler size on thermophysical and electrical behavior of nanocomposites based on expanded graphite nanoparticles filled in low-density polyethylene matrix. *Polym. Compos.* **2013,** 34, (2), 149-155.
38. Wu, S.-H.; Masaharu, I.; Natsuki, T.; Ni, Q.-Q. Electrical Conduction and Percolation Behavior of Carbon Nanotubes/UPR Nanocomposites. *J. Reinf. Plast. Compos.* **2006,** 25, (18), 1957-1966.
39. Chen, L.; Lu, L.; Wu, D.; Chen, G. Silicone rubber/graphite nanosheet electrically conducting nanocomposite with a low percolation threshold. *Polym. Compos.* **2007,** 28, (4), 493-498.
40. Zeng, X.; Xu, X.; Shenai, P. M.; Kovalev, E.; Baudot, C.; Mathews, N.; Zhao, Y. Characteristics of the Electrical Percolation in Carbon Nanotubes/Polymer Nanocomposites. *TJ. Phys. Chem. C* **2011,** 115, (44), 21685-21690.
41. Zhuo, M.; Grazioli, D.; Simone, A. Active material utilization and capacity of fiber-based battery electrodes. *Electrochim. Acta* **2020,** 333, 134929.
42. Balberg, I.; Binenbaum, N. Computer study of the percolation threshold in a two-dimensional anisotropic system of conducting sticks. *Phys. Rev. B* **1983,** 28, (7), 3799-3812.
43. Ni, X.; Hui, C.; Su, N.; Cutler, R.; Liu, F. A 3D percolation model for multicomponent nanocarbon composites: the critical role of nematic transition. *Nanotechnology* **2019,** 30, (18), 185302.
44. Tarasevich, Y. Y.; Eserkepov, A. V. Percolation of sticks: Effect of stick alignment and length dispersity. *Phys. Rev. E* **2018,** 98, (6), 062142.
45. Luo, Z.; Li, X.; Li, Q.; Tian, X.; Fan, T.; Wang, C.; Wu, X.; Shen, G. In Situ Dynamic Manipulation of Graphene Strain Sensor with Drastically Sensing Performance Enhancement. *Adv. Electron. Mater.* **2020,** 6, (6), 2000269.
46. Dang, Z.-M.; Jiang, M.-J.; Xie, D.; Yao, S.-H.; Zhang, L.-Q.; Bai, J. Supersensitive linear piezoresistive property in carbon nanotubes⁄silicone rubber nanocomposites. *J. Appl. Phys.* **2008,** 104, (2), 024114.
47. Jiang, M.-J.; Dang, Z.-M.; Xu, H.-P.; Yao, S.-H.; Bai, J. Effect of aspect ratio of multiwall carbon nanotubes on resistance-pressure sensitivity of rubber nanocomposites. *Appl. Phys. Lett.* **2007,** 91, (7), 072907.
48. Lee, T.; Lee, W.; Kim, S.-W.; Kim, J. J.; Kim, B.-S. Flexible Textile Strain Wireless Sensor Functionalized with Hybrid Carbon Nanomaterials Supported ZnO Nanowires with Controlled Aspect Ratio. *Adv. Funct. Mater.* **2016,** 26, (34), 6206-6214.
49. Yao, H.; Hempel, M.; Hsieh, Y.-P.; Kong, J.; Hofmann, M. Characterizing percolative materials by straining. *Nanoscale* **2019,** 11, (3), 1074-1079.
50. Backes, C.; Abdelkader, A. M.; Alonso, C.; Andrieux-Ledier, A.; Arenal, R.; Azpeitia, J.; Balakrishnan, N.; Banszerus, L.; Barjon, J.; *et al.* Production and processing of graphene and related materials. *2D Mater.* **2020,** 7, (2), 022001.
51. De, S.; King, P. J.; Lyons, P. E.; Khan, U.; Coleman, J. N. Size effects and the problem with percolation in nanostructured transparent conductors. *ACS Nano* **2010,** 4, (12), 7064-72.
52. Coleman, J. N.; Curran, S.; Dalton, A. B.; Davey, A. P.; McCarthy, B.; Blau, W.; Barklie, R. C. Percolation-dominated conductivity in a conjugated-polymer-carbon-nanotube composite. *Phys. Rev. B* **1998,** 58, (12), R7492-R7495.
53. Saeed, K.; Park, S.-Y. Preparation and properties of multiwalled carbon nanotube/polycaprolactone nanocomposites. *J. Appl. Polym. Sci.* **2007,** 104, (3), 1957-1963.

54. Zhou, P.; Liao, Y.; Li, Y.; Pan, D.; Cao, W.; Yang, X.; Zou, F.; Zhou, L.-m.; Zhang, Z.; Su, Z. An inkjet-printed, flexible, ultra-broadband nanocomposite film sensor for in-situ acquisition of high-frequency dynamic strains. *Composites, Part A* **2019,** 125, 105554.
55. Wang, X.; Li, J.; Song, H.; Huang, H.; Gou, J. Highly Stretchable and Wearable Strain Sensor Based on Printable Carbon Nanotube Layers/Polydimethylsiloxane Composites with Adjustable Sensitivity. *ACS Appl. Mater. Interfaces* **2018,** 10, (8), 7371-7380.
56. Wang, X.; Sparkman, J.; Gou, J. Strain sensing of printed carbon nanotube sensors on polyurethane substrate with spray deposition modeling. *Comp. Comm.* **2017,** 3, 1-6.
57. Casiraghi, C.; Macucci, M.; Parvez, K.; Worsley, R.; Shin, Y.; Bronte, F.; Borri, C.; Paggi, M.; Fiori, G. Inkjet printed 2D-crystal based strain gauges on paper. *Carbon* **2018,** 129, 462-467.
58. Bonaccorso, F.; Bartolotta, A.; Coleman, J. N.; Backes, C. 2D-Crystal-Based Functional Inks. *Adv. Mater.* **2016,** 28, (29), 6136-6166.
59. Torrisi, F.; Carey, T. Graphene, related two-dimensional crystals and hybrid systems for printed and wearable electronics. *Nano Today* **2018,** 23, 73-96.
60. Kelly, A. G.; Hallam, T.; Backes, C.; Harvey, A.; Esmaeily, A. S.; Godwin, I.; Coelho, J.; Nicolosi, V.; Lauth, J.; Kulkarni, A.; *et al.* All-Printed Thin-Film Transistors from Networks of Liquid-Exfoliated Nanosheets. *Science* **2017,** 356, (6333), 69-73.
61. Coleman, J. N.; Khan, U.; Blau, W. J.; Gun'ko, Y. K. Small but Strong: A Review of the Mechanical Properties of Carbon Nanotube-Polymer Composites. *Carbon* **2006,** 44, (9), 1624-1652.

Figures

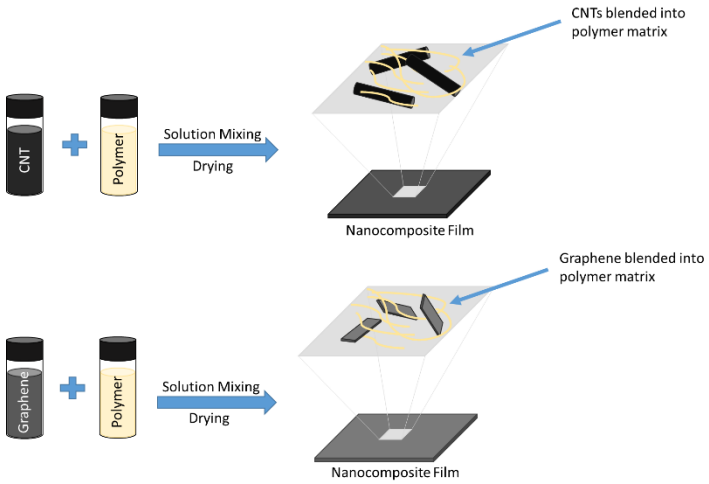

Figure 1. Schematic illustration of a common method of mixed-phase nanocomposite production

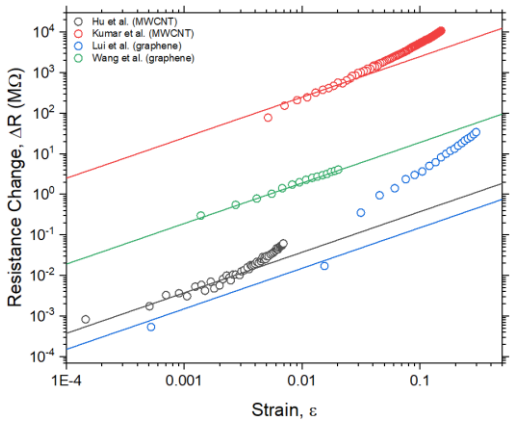

Figure 2. Literary data fitted using eq 10. The expression is found to fit the data sets accurately in the low strain linear regime. See Supporting Information Table S1 for fit parameters.

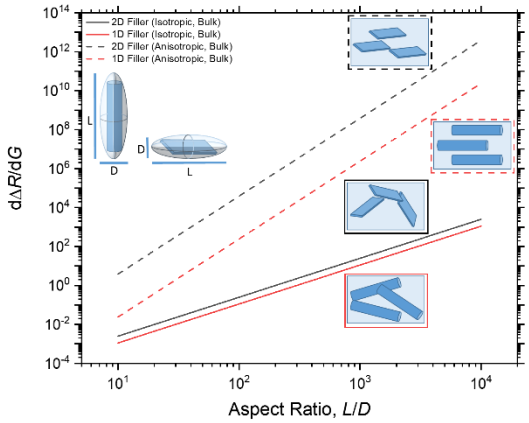

Figure 3. Modelling electrometrical response of bulk isotropic and anisotropic nanocomposites from eq 14. As predicted by eq 8, anisotropic nanocomposites with nanofillers aligned in-plane with current flow displayed a larger response in comparison to the isotropic counterpart. At an aspect ratio of 1000, the 2D anisotropic system had a response eight orders of magnitude larger than the isotropic one. In general, nanocomposites based on 2D nanofillers are found to have better performance than 1D nanofillers in a comparable system. Inset top left, 1D and 2D nanofillers modelled as ellipsoids with aspect ratios defined by length *L* and diameter *D*.

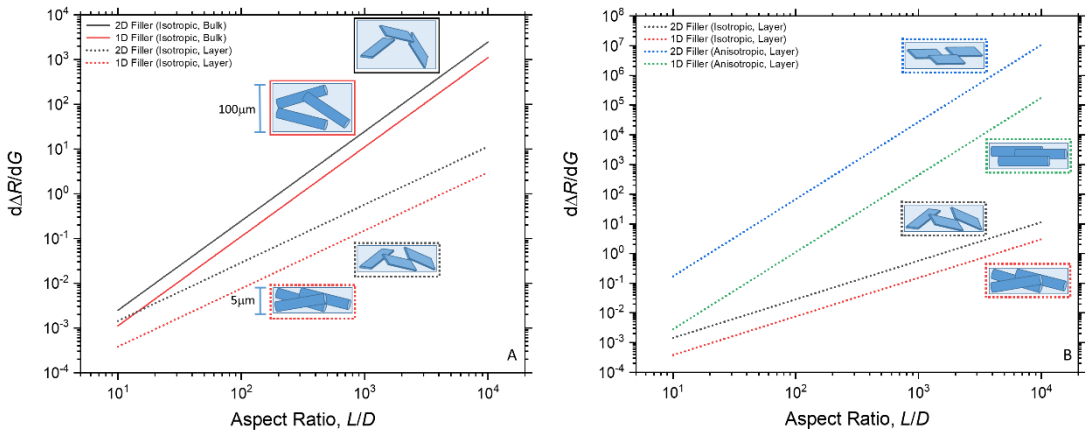

Figure 4. (A) From eq 14, a comparison between the bulk isotropic system ($L_{0,Bulk}$ = 100 μm) and an equivalent thinner layer system ($L_{0,layer}$ = 5μm) is shown. At a nominal aspect ratio of 1000, the bulk isotropic system presents a better electromechanical response. However, when approaching aspect ratios <100 the performances begin to converge towards similar values. As noted previously, 2D nanofillers display a larger overall response than 1D materials. (B) The effect of anisotropy on the layer system again sees a dramatic increase in electromechanical response with respect to the isotropic systems. At an aspect ratio of 1000, the anisotropic 2D system was found to have a response about five orders of magnitude larger that the isotropic one.

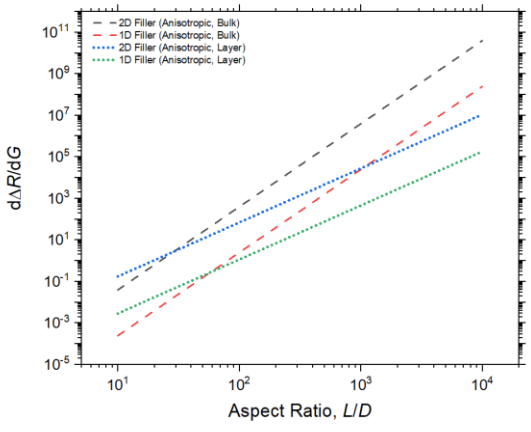

Figure 5. Comparing the anisotropic bulk and thin layer systems sees both systems performing similarly at low aspect ratios (<100). However, at larger aspect ratios, more indicative of experimental values, the bulk systems were found to outperform the thinner layer systems.

TOC Graphic

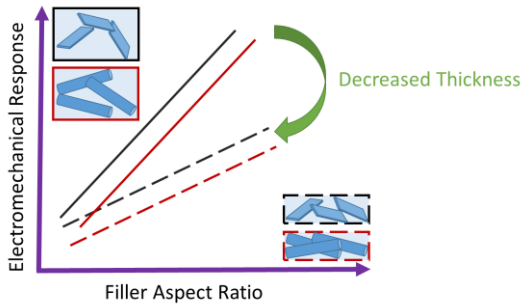
Electromechanical Response
Filler Aspect Ratio
Decreased Thickness